Parallel purine–pyrimidine–purine triplex: experimental evidence for existence

Anna K. Shchyolkina, Olga F. Borisova, Elvira E. Minyat, Edward N. Timofeev, Irina A. Il'icheva, Elena B. Khomyakova, Vladimir L. Florentiev*

V.A. Engelhardt Institute of Molecular Biology, Russian Academy of Sciences, Vavilova str. 32, 117984 Moscow, Russian Federation

Received 24 April 1995

Abstract **Oligonucleotides 5′-d(CT)$_5$-L-d(AG)$_5$-L-d(GA)$_5$-3′ and 5′-d(GA)$_5$-L-d(TC)$_5$-L-d(GA)$_5$-3′ [L = pO(CH$_2$CH$_2$O)$_3$p] were studied by thermal denaturation, chemical modification and binding of fluorescent dyes. Both oligonucleotides are shown to fold back on itself twice forming at pH 7 a sufficiently stable triplex ether with antiparallel-oriented oligopurine strands (the first compound) or parallel-oriented oligopurine strands (the second compounds). The parallel triplex is significantly less stable than the antiparallel one. On the basis of conformational modeling, possible types of base tripling in the triplets are proposed. Thus our data provide the first convincingly evidence for the existence of a purine–pyrimidine–purine triplex with parallel orientation of identical strands.**

Key words: Parallel DNA triplex; Purine–pyrimidine–purine sequence; Relative stability; Base tripling

1. Introduction

The exploitation of DNA triple helix formation is for the time being the most versatile and rational approach to sequence-specific DNA recognition. Triplex forming oligonucleotides were shown to can be potentially used as sequence-specific artificial nucleases [1], modulators of DNA-binding protein [2,3], regulators of gene expression [4,5] and subsequently as therapeutical agents [6,7]. A specific feature of such triplexes is the requirement for homopurine–homopyrimidine tract in target DNA sequence. The third strand can be either homopyrimidine (Py–Pu–Py triplexes) or homopurine (Py–Pu–Pu triplexes) but in both cases the third strand is antiparallely oriented with respect to the identical strand of duplex. We call such triplexes antiparallel or 'classical' triplexes. On the other hand triplexes with parallel-oriented identical strands (parallel triplexes) were shown recently to form as intermediates during homologous recombination promoted by RecA and some other recombinase proteins [8,9]. It is very important to study possibility of protein-independent formation of parallel triplexes and comparison of their properties with properties of antiparallel triplexes. We present here the first experimental evidence for formation of a Py–Pu–Pu triplex with parallel orientation of identical (purine) strands (parallel triplex).

The d(TC)$_n$–d(AG)$_n$–d(AG)$_n$ triplexes were chosen because d(TC)$_n$–d(AG)$_n$ sequences were found at unexpectedly high levels in eukaryotic genomes [10]. All TC–AG–AG triplexes studied to date belong to antiparallel type [11–17]. To investigate the possibility of existence of TC–AG–AG parallel triplexes we used the 'forced strand orientation' approach proposed by us earlier [18]. This approach which was successfully applied to investigate triplexes with various direction of strands [19,20] centres on compounds consisting of three oligonucleotide segments coupled by hydroxyalkyl chains of an appropriate length. In this study we present experiments probing the structure, stability, and thermodynamics of two synthetic oligonucleotides 5′ d(CT)$_5$-pO(CH$_2$CH$_2$O)$_3$p-d(AG)$_5$-pO(CH$_2$CH$_2$O)$_3$-p-d(GA)$_5$ **(I)** and 5′d(GA)$_5$-pO(CH$_2$CH$_2$O)$_3$p-d(TC)$_5$-pO-(CH$_2$CH$_2$O)$_3$p-d(GA)$_5$ **(II)**. Both oligomers are able to fold back on itself twice to form intramolecular triplexes either with antiparallel (oligonucleotide **I**) or parallel (oligonucleotide **II**) orientation of identical strands (see Fig. 1).

2. Materials and methods

The oligonucleotides 5′ d(CT)$_5$-pO(CH$_2$CH$_2$O)$_3$p-d(AG)$_5$-pO-(CH$_2$CH$_2$O)$_3$p-d(GA)$_5$ **(I)** and 5′d(GA)$_5$-pO(CH$_2$CH$_2$O)$_3$p-d(TC)$_5$-pO(CH$_2$CH$_2$O)$_3$p-d(GA)$_5$ **(II)** were synthesized by the phosphite triester method on a solid-phase carrier from 3′-phosphoramidites of protected nucleotides and 1-*O*-dimethoxytrityl-10-*O*-(*N*-diisopropylaminomethoxyphosphinyl)-1,8-dihydroxy-3,6-dioxaoctane. Partly deblocked 5′-dimethoxytrityl oligonucleotide was isolated by the reverse phase HPLC. After treatment with acetic acid, the reaction product was purified by the ion exchange HPLC and finally desalted and concentrated by gel filtration.

All solutions were prepared in 0.01 M Na-phosphate buffer, pH 7.0. The oligonucleotide solutions were annealed by heating up to 90°C with subsequent slow cooling. Concentrations of oligonucleotides were determined by UV spectra, assuming the extinction coefficient, ε_{260}, to be equal to 11,300 $M^{-1} \cdot cm^{-1}$ per 1 mol of nucleotides at 90°C.

Melting curves were registered with a Beckman spectrophotometer (USA) at 260 nm in a thermostatic cuvette with the optical path length of 1 cm. The heating rate was constant and equal to 0.2°C/min.

The fluorescent polarization, P, was monitored with an AMINCO SPF 1000 (USA) spectrofluorometer in thermostatic cuvettes at temperatures from 3 to 10°C. The rotation relaxation time, ρ, was calculated by the following equation:

$$\rho = 3\tau(1/P_o - 1/3)/(1/P - 1/P_o), \quad (1)$$

where τ is the time of fluorescent quenching (τ = 25 ns at 3°C), P_o is the limit value of P at $T/\eta \rightarrow 0$(P_o = 0.42), η is the viscosity of the solution, and T is absolute temperature [21].

Sequencing was carried out by the routine procedure [22]. Chemical modification and enzymatic digestion were performed at 0–3°C by the methods previously described [23]. The autoradiograms were scanned down the lanes with a 300A Computing Densitometer (Molecular Dynamics, USA).

Conformational energy minimization was performed with the AMBER 3.0 program [24]. No water molecules were explicitly taken into account, but their effect was simulated by use of a distance-dependent dielectric constant.

*Corresponding author. Fax: (7) (095) 135 14 05.

SSDI 0014-5793(95)00519-6

3. Results and discussion

The melting curves of oligonucleotides **I** and **II** have pronounced biphasic character (Fig. 2). The two cooperative transitions are indicative of the formation of a multistranded structures at low temperatures. If these structures are intramolecular, they can only be triplexes. To determine whether low-temperature complexes are intramolecular, we calculated relative hydrodynamic volume of these structures via the fluorescent polarization of intercalated ethidium bromide by the method proposed by us previously [25]. Ethidium bromide intercalates between hydrogen-bonded duplex or triplex layers. In the case of compounds consisting of oligonucleotide units bound by flexible hinges, this method reveals the relative volume (the ratio of the volume of compound studied to the volume of reference $d(CCGGATCCGG)_2$ duplex) of the paired or tripled part of the molecule (for example, the relative volume of hairpin with dangling third segment is close to 1). We found that at 3°C in the presence 0.1 M NaCl the relative volume of oligonucleotides **I** and **II** are 1.40 ± 0.05 and 1.45 ± 0.1 respectively. These data indicate conclusively that both oligonucleotide **I** and oligonucleotide **II** are folded into intramolecular triplexes with antiparallel **(apTR)** or parallel **(pTr)** direction of identical strands (Fig. 1). It is interesting to note that both antiparallel and parallel triplex tend to self-association at increasing of strand concentration or ionic strength and particularly at addition of Mg^{2+}. So, in the presence if 1 mM Mg^{2+} the relative volume of oligonucleotides **I** and **II** are 2.0 ± 0.1 and 2.3 ± 0.1, respectively, which indicates an almost complete dimerisation of these triplexes.

Additional evidence for the triplex formation is provided by chemical probing (Fig. 3). In the case of triplex formation from a single-stranded oligonucleotide and a longer duplex, the criterion of triplex existence is that the part of the duplex covered by the third strand is modified to a lesser degree than the uncovered parts thereof. We used model compounds wherein all nucleotides were involved into the triplex structure. In this

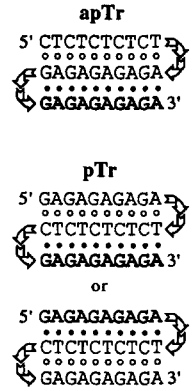

Fig. 1. Topology of folding of oligonucleotide **I(apTr)** and oligonucleotide **II(pTr)**.

case, a more pronounced modification of bases located at the triplex ends unambiguously indicate protection against chemical modification and hence triplex formation. As can be seen in Fig. 3 (lanes of DEP and OsO_4), all three oligonucleotide segments of oligonucleotide **I** and **II** are protected against chemical modification (the boundaries between segments are easily determined by increased distance between bands because extrusion of 3′ terminal nucleoside in the central or 5′ terminal oligonucleotide segments decrease the charge of 5′ labeled oligonucleotide by two units at once).

The patterns of S1 nuclease digestion of **apTr** and **pTr** are shown in Fig. 3 (S1 lanes). The fact that there are only ten bands in the 3′ segment part of the pattern indicates that S1 nuclease cleaves the 5′-NpL linkage but not the 5-LpN linkage (L–hydroxyalkyl linker). It is important to note that labeled oligonucleotides of a certain length obtained by nuclease digestion possess lesser electrophoretic mobility than oligonucleotides of the same length obtained by chemical modification due to the absence of 3′ terminal phosphate. In the case of **apTr** all three segments are protected against S1 degradation. The

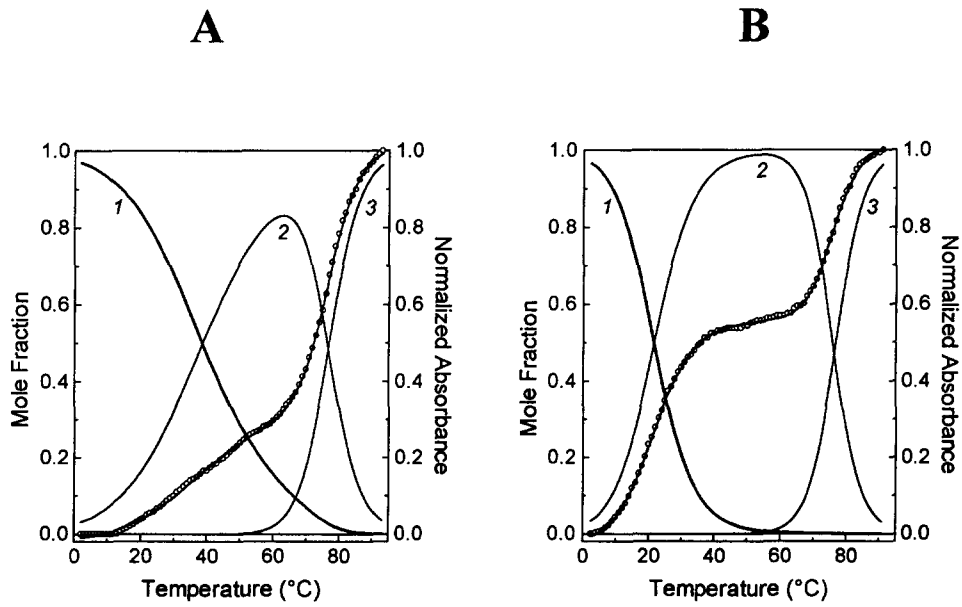

Fig. 2. Experimental (circles) and modeling (straight line) melting curves and calculated mole fraction of triplex (*1*), duplex (*2*) and open strand (*3*) of **apTr(A)** and **pTR(B)** in 0.01 M Na phosphate buffer, pH 7, at 0.25 M NaCl. Concentrations of oligonucleotides were 2×10^{-5} M of nucleotides.

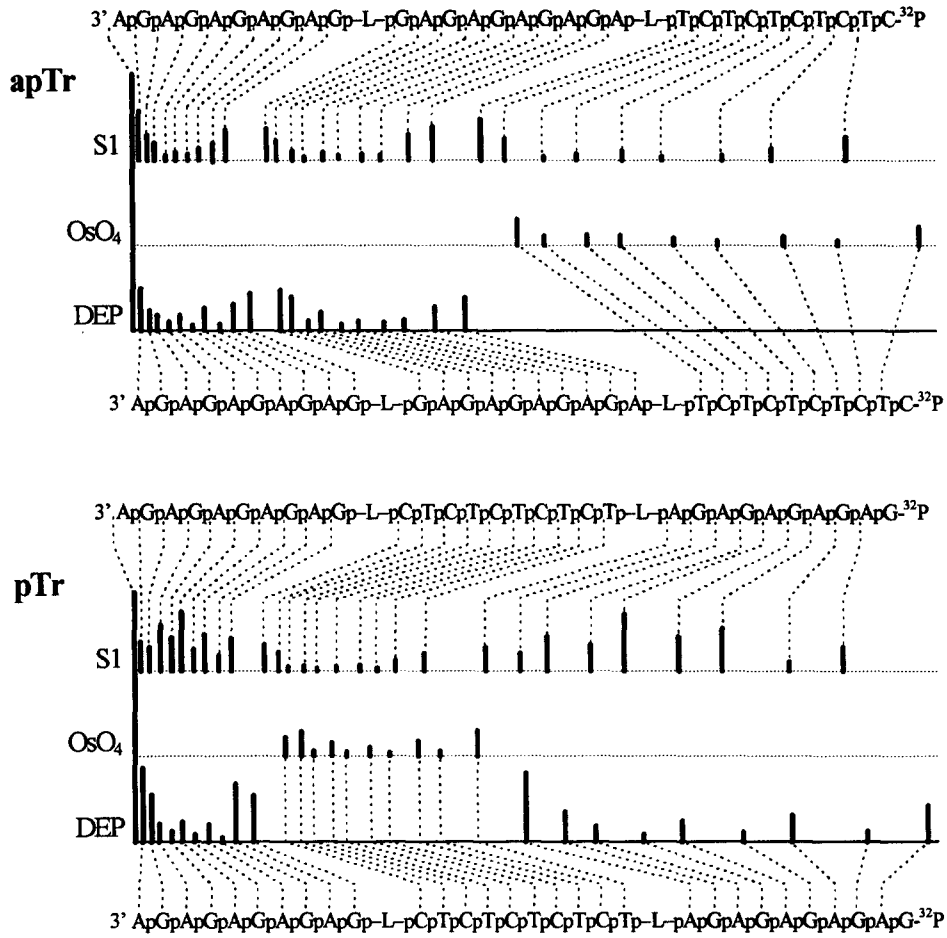

Fig. 3. Densitograms of chemical modification with diethylpyrocarbonate (DEP) and osmium tetraoxyde (OsO_4) and nuclease digestion (S1). The peaks of densitograms are presented as bars which height is equal to the integrated peak area. The probing was carried out at 3°C as described previously [23].

3′ homopurine segment undergoes a slightly more intensive cleavage than two others. As for the chemical modification, the ends of a triplex are more sensitive to nuclease digestion. Such type of degradation fully corresponds to the expected structure of **apTr**. Indeed, the **apTr** can exist only as one isomer (see Fig. 1). Due to the chemical structure of oligonucleotide **I**, the 3′ segment must be the third (non-Watson–Crick) strand of the triplex.

The pattern for **pTr** is dramatically different from the pattern for **apTr**. First, oligopurine segments of **pTr** are more susceptible to S1 nuclease than those of **apTr**. Second, the degree of degradation increases gradually from the ends to the center of

Table 1
Thermodynamic parameters* of structural transitions of oligonucleotides **I** and **II**

Oligonucleotide	Condition†	Triplex-to-duplex transition			Duplex-to-open strand transition		
		$\Delta H°$ (kcal/mol)	$\Delta S°$ (cal·mol^{-1}·K^{-1})	T_m (°C)	$\Delta H°$ (kcal/mol)	$\Delta S°$ (cal·mol^{-1}·K^{-1})	T_m (°C)
I	0 M NaCl	32.9	108.0	31.6	52.5	155.6	64.4
	0.25 M NaCl	31.6	101.2	39.2	48.8	139.6	76.6
	1.0 M NaCl	31.2	98.0	45.3	44.8	125.7	83.4
	0.01 M Mn^{2+}	26.9	88.3	31.6	52.2	151.3	72.0
II	0 M NaCl	26.4	90.7	18.2	53.9	160.3	63.2
	0.25 M NaCl	27.8	94.3	21.8	47.6	136.4	76.0
	1.0 M NaCl	29.8	96.9	33.9	46.1	130.2	81.2
	0.01 M Mn^{2+}	19.6	65.1	27.9	50.5	147.0	70.5

Thermodynamic parameters were calculated from the melting curves in the three states model by the method previously described [20].
*Errors are ±2 kcal/mol for $\Delta H°$; ±6 cal·mol^{-1}·K^{-1} for $\Delta S°$; ±1°C for T_m.
†To the initial solution containing oligonucleotide in 0.01 M Na phosphate buffer, pH 7, NaCl, or $MnCl_2$ was added (final concentration of oligonucleotide was about 2×10^{-5} M of nucleotides).

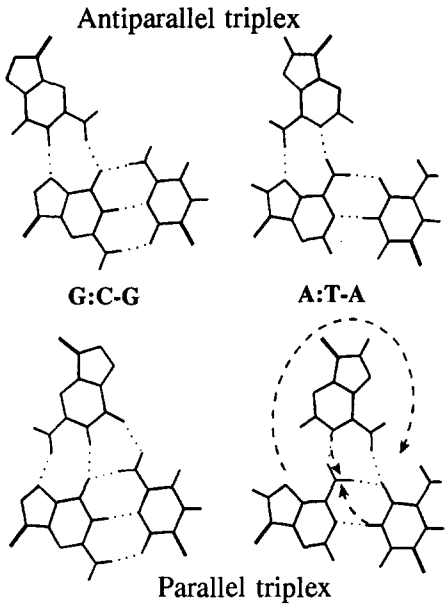

Fig. 4. Base-pairing schemes in the antiparallel and parallel pyrimidine-purine-purine triplexes. Dotted arrows in bottom right structure show the possible movement of bases at topoisomer interconvertion.

$(AG)_5$ segments. Third, a greater sensitivity of 5′ GpA linkages as compared with 5′ ApG linkages is manifested. The above features of S1 digestion were shown earlier [26] to be characteristic of single-stranded $(AG)_n$ sequences. Such type of pattern would indicate the absence of a three-stranded structure if only one of two $(AG)_5$ segments were cleaved in such a way. However, the fact that both homopurine segments of **pTr** are digested approximately equally but the oligopyrimidine segment is fully protected not only proves existence of a parallel triplex but also interconvertion of two possible topoisomers shown in Fig. 1. Indeed, as it can be seen from the scheme of hydrogen bonding of bases in the parallel triplex (Fig. 4), a probable route for interconversion of isomers is that pyrimidine bases of the Watson–Crick duplex and purine bases of the third strand turn towards each other to form new Watson–Crick duplex. The other purine strand falls within the minor groove of this duplex and is superseded from the triplex. After dislocation of this strand into the major groove of the duplex, the triplex is formed again. Therefore both homopurine strands become by turn in single-stranded state while oligopyrimidine strand always is involved in the Watson–Crick duplex.

The triple-stranded DNA with parallel-oriented identical strands has been recently shown to be intermediate during homologous recombination promoted by RecA protein [8,9]. The isomers interconversion detected by us probably simulates the strand exchange in the general recombination.

The thermodynamic parameters of **apTr** and **pTr** formation were calculated from the melting curves (Table 1). As seen from these data, the parallel triplex is significantly less stable than the antiparallel one. It is not difficult to evaluate the ratio of fractions of parallel and antiparallel triplexes when parallel and antiparallel triplexes can be formed simultaneously. This ratio can be calculate with equation $\exp(-\Delta\Delta G^\circ/RT)$, where $\Delta\Delta G^\circ$ is difference of standard free energies of parallel and antiparallel triplex formation. As seen from Table 1 in 0.25 M NaCl, $\Delta\Delta G^\circ$ is equal to 1.92 kcal/mol at 0°C and 1.74 kcal/mol at 25°C. The fractions of parallel triplex will be only 3 and 5%, correspondingly. This fact could probably explain why only antiparallel triplexes were registered to date.

Acknowledgements: This work was supported by International Science Foundation (Grant M6X000), Russian Foundation for Fundamental Investigation and Russian National Program for Novel Biotechnology Methods.

References

[1] Strobel, S.A., Doucettestamm, L.A., Riba, L., Housman, D.E. and Dervan, P.B. (1991) Science 254, 1639–1642.
[2] Gee, J.E., Blume, S., Snyder, R.C., Ray, R. and Miller, D.M. (1992) J. Biol. Chem. 267, 1163–1167.
[3] Ebbinghaus, S.W. and Miller, D.M. (1991) Clin. Res. 39, 863–868.
[4] Maher, L.J. (1992) Biochemistry 31, 7587–7594.
[5] Duvalvalentin, G., Thuong, N.T. and Helene, C. (1992) Proc. Nat. Acad. Sci. USA 89, 504–508.
[6] Helene, C. (1991) Anti-Cancer Drug Design 6, 569–584.
[7] Chubb, J.M. and Hogan, M.E. (1992) Trends Biotechnol. 10, 132–136.
[8] Hsieh, P., Camerini-Otero, C.S. and Camerini-Otero, R.D. (1990) Genes Dev. 4, 1951–1963.
[9] Rao, B.J., Chiu, S.K. and Radding, C.M. (1993) J. Mol. Biol. 229, 328–343.
[10] Wells, R.D., Collier, D.A., Harvey, J.C., Shimizu, M. and Wohlrab, F. (1988) FASEB J. 2, 2939–2949.
[11] Bernues, J., Beltran, R., Casasanovas, J. and Azorin, F. (1989) EMBO J. 8, 2087–2094.
[12] Bernues, J., Beltran, R., Casasanovas, J.M. and Azorin, F. (1990) Nucleic Acids Res. 18, 4067–4073.
[13] Chen, F.M. (1991) Biochemistry 30, 4472–4479.
[14] Malkov, V.A., Voloshin, O.N., Soyfer, V.N. and Frank-Kamenetskii, M.D. (1993) Nucleic Acids Res. 21, 585–591.
[15] Malkov, V.A., Soyfer, V.N. and Frank-Kamenetskii, M.D. (1992) Nucleic Acids Res. 20, 4889–4895.
[16] Lyamichev, V.I., Voloshin, O.N. and Frank-Kamenetskii, M.D. (1991) Nucleic Acids Res. 19, 1633–1638.
[17] Kan, L.S., Callahan, D.E., Trapane, T.L., Miller, P.S., Tso, P.O.P. and Hugan, D.H. (1991) J. Biomol. Struct. Dynam. 8, 911–933.
[18] Shchyolkina, A.K., Lysov, Yu.P., Il'icheva, I.A., Chernyi, A.A., Golova, Yu.B., Chernov, B.K., Gottikh, B.P. and FLorentiev, V.L. (1989) FEBS Lett. 244, 39–42.
[19] Shchyolkina, A.K., Timofeev, E.N., Borisova, O.F., Il'icheva, I.A., Minyat, E.E., Khomyakova, E.B. and Florentiev, V.L. (1994) FEBS Lett. 339, 113–118.
[20] Shchyolkina, A.K., Mamayeva, O.K., Borisova, O.F., Lysov, Yu.P., Timofeev, E.N., Il'icheva, I.A., Gottikh, B.P. and Florentiev, V.L. (1994) Antisence Res. Dev. 4, 28–33.
[21] Borisova, O.F., Golova, Yu.B., Gottikh, B.P., Zibrov, A.S., Il'icheva, I.A., Lysov, Yu.P., Mamayeva, O.K., Chernov, B.K., Chernyi, A.A., Shchyolkina, A.K. and Florentiev, V.L. (1991) J. Biomol. Struct. Dynam. 8, 1187–1210.
[22] Maxam, A.M. and Gilbert, W. (1980) Methods Enzymol. 65, 499–559.
[23] Gogoshidze, M.Z., Minyat, E.E., Gorin, A.A., Demchuk, E.Ya., Farutin, V.A. and Ivanov, V.I. (1992) Mol. Biol. (Russ.) 26, 1263–1273.
[24] Singh, U.C., Weiner, P.K., Caldwell, J.W., Kollman, P.A., AMBER (UCSF), version 3.0, Department of Pharmaceutical Chemistry, University of California: San Francisco, 1986.
[25] Borisova, O.F., Golova, Yu.B., Gottikh, B.P., Zibrov, A.S., Il'icheva, I.A., Lysov, Yu.P., Mamaeva, O.K., Chernov, B.K., Chernyi, A.A., Shchyolkina, A.K. and Florentiev, V.L. (1991) J. Biomol. Struct. Dynam. 8, 1187–1210.
[26] Pulleyblank, D.E., Glover, M., Farah, C. and Haniford, B. (1988) in: Unusual DNA Structures (Welss, R.D. and Harvey, S.C., Eds.) pp. 23–44, Springer-Verlag, New York.